



## Research paper

# pySCu: A new python code for analyzing remagnetizations directions by means of small circle utilities



Pablo Calvin<sup>a,\*</sup>, Juan J. Villalaín<sup>a</sup>, Antonio M. Casas-Sainz<sup>b</sup>, Lisa Tauxe<sup>c</sup>, Sara Torres-López<sup>a</sup>

<sup>a</sup> Dep. de Física, Lab. de Paleomagnetismo, Universidad de Burgos, Spain

<sup>b</sup> Dep. de Ciencias de la Tierra, Universidad de Zaragoza, Spain

<sup>c</sup> Scripps Institution of Oceanography, University of California San Diego, La Jolla, CA 92093-0220, USA

## ARTICLE INFO

## Keywords:

Small circle  
SCI method  
Fold-test  
Remagnetization  
Synfolding  
pySCu

## ABSTRACT

The Small Circle (SC) methods are founded upon two main starting hypotheses: (i) the analyzed sites were remagnetized contemporarily, acquiring the same paleomagnetic direction. (ii) The deviation of the acquired paleomagnetic signal from its original direction is only due to tilting around the bedding strike and therefore the remagnetization direction must be located on a small circle (SC) whose axis is the strike of bedding and contains the in situ paleomagnetic direction. Therefore, if we analyze several sites (with different bedding strikes) their SCs will intersect in the remagnetization direction.

The SC methods have two applications: (1) the Small Circle Intersection (SCI) method is capable of providing adequate approximations to the expected paleomagnetic direction when dealing with synfolding remagnetizations. By comparing the SCI direction with that predicted from an apparent polar wander path, the (re)magnetization can be dated. (2) Once the remagnetization direction is known, the attitude of the beds (at each site) can be restored to the moment of the acquisition of the remagnetization, showing a palinspastic reconstruction of the structure. Some caveats are necessary under more complex tectonic scenarios, in which SC-based methods can lead to erroneous interpretations. However, the graphical output of the methods tries to avoid 'black-box' effects and can minimize misleading interpretations or even help, for example, to identify local or regional vertical axis rotations. In any case, the methods must be used with caution and always considering the knowledge of the tectonic frame.

In this paper, some utilities for SCs analysis are automatized by means of a new Python code and a new technique for defining the uncertainty of the solution is proposed. With pySCu the SCs methods can be easily and quickly applied, obtaining firstly a set of text files containing all calculated information and subsequently generating a graphical output on the fly.

## 1. Introduction

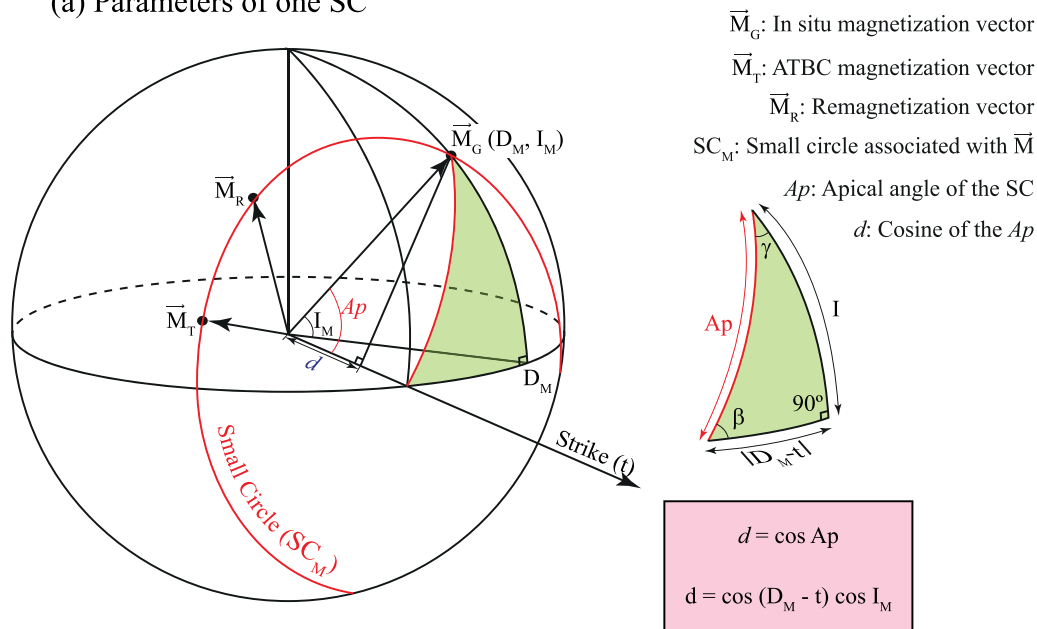
The paleomagnetic fold-test (Graham, 1949) is a basic tool for recognizing pre-, syn- or post-folding magnetizations. However, for structural reconstructions using synfolding remagnetizations (defining "synfolding" as either a magnetization acquired between two different folding events -i.e. between the end of the first folding stage and before the beginning of the second one, or during the development of a fold in a single event-) this method cannot be used because the incremental fold-test (McCabe and Elmore, 1989; McFadden, 1990; Bazhenov and Shipunov, 1991; Watson and Enkin, 1993; Tauxe and Watson, 1994) assumes proportional folding at the different limbs and this is an assumption not necessarily met in nature (e.g. Suppe, 1983; Cairanne

et al., 2002; Delaunay et al., 2002; Villalaín et al., 2003).

To overcome the (sometimes) erroneous assumption of proportional folding and to obtain the correct restoration of bedding, some authors proposed more detailed analyses with non-symmetric unfolding of the different fold limbs. These efforts are based on the fact that the transformation of a paleomagnetic vector from geographic to stratigraphic coordinates (i.e. tilt correction) implies the rotation of the vector along a small circle (SC) whose axis is the strike of the bed and the amount of rotation is the dip angle. In this way, McClelland-Brown (1983) treated synfolding remagnetizations by comparing different percentages of unfolding of the limbs and analyzing the path of the paleomagnetic direction upon the corresponding SC. Surmont et al. (1990) observed maximum clustering of the paleomagnetic direction after applying partial

\* Corresponding author. Dep. Física, Escuela Politécnica Superior, Río Vena, Universidad de Burgos, Av. Cantabria s/n, 09006 Burgos, Spain.  
E-mail address: [calvinballester@gmail.com](mailto:calvinballester@gmail.com) (P. Calvin).

(a) Parameters of one SC



(b) P, Q and angular distance ( $\alpha$ ) between P and SC

$SC_M$ : Small circle whose axis is 't' and contains  $\bar{M}$   
 Q: nearest point between P and  $SC_M$

Looking perpendicular to the great circle in which P and strike are (the green one)

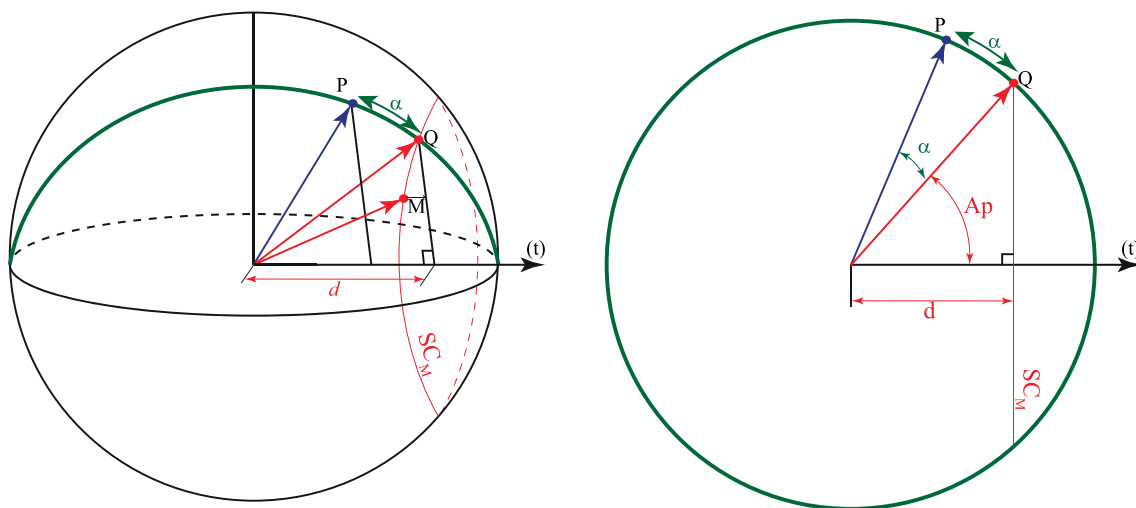


**Fig. 1.** (a) A small circle (SC) associated with one paleomagnetic site is defined by the strike of the bedding ( $t$ ) and by the direction of the magnetization ( $M$ ) and therefore it can be parametrized by  $t$  and the apical angle ( $Ap$ ) of the SC which is equal to the angle between the magnetization and strike vectors. Working in a unit sphere,  $Ap$  can be defined by its cosine  $d$ . (b)  $\alpha$  is the minimum angular distance between the given direction P and the  $SC_M$  and is defined as the angle between P and Q, the latter being the intersection between the  $SC_M$  and the great circle that contains P and  $t$ .

tilt corrections at the sites (i.e. the space region showing higher concentration of intersection between the SC); they considered this cluster as the remagnetization direction and the discrepancy with the expected direction was attributed to vertical axis rotation. A similar work was presented by Villalaín et al. (1992) who calculated a local remagnetization direction as intersection of the SCs and restored each limb separately.

An important forward step was done by Shipunov (1997) who clearly established the Small Circle Intersection (SCI) as a useful method to calculate local remagnetization directions. When the paleomagnetic direction corresponds with a synfolding remagnetization (i.e. the

magnetization was acquired after partial folding of beds) and supposing only tilting of the beds around a horizontal axis (e.g. absence of differential vertical axis rotation between each paleomagnetic site), the actual local direction of the remagnetization must be coincident for all sites and located along each SC. In other words, the small circles must show a common direction (or narrow spatial distribution), corresponding to the local direction of the remagnetization (Shipunov, 1997).

More improvements for the SCI method were made by Henry et al. (2004), who established the reliability of the method depending on the geological conditions (e.g. the distribution of strikes of the beds), and modified the way to calculate the remagnetization direction. They also

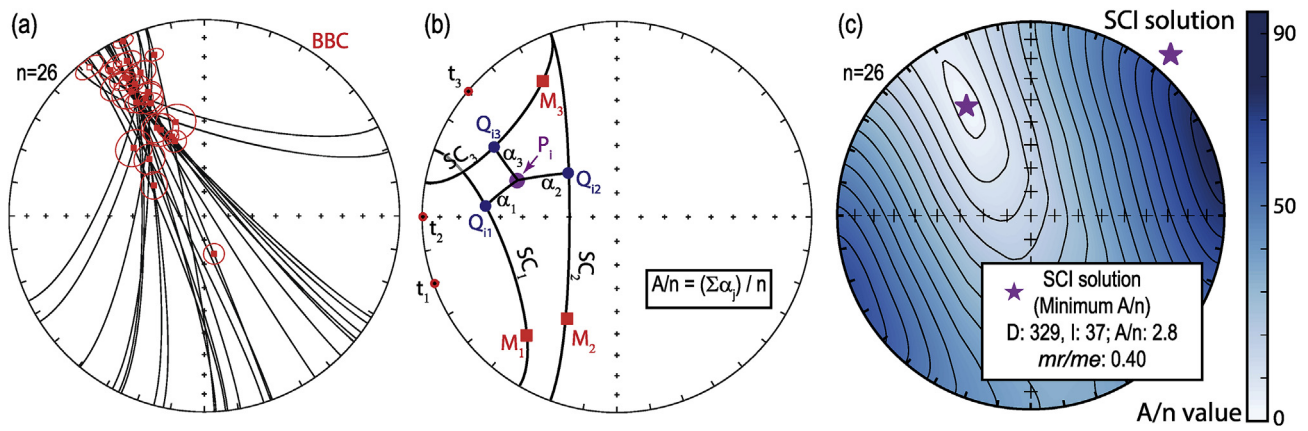


**Fig. 2.** Lower hemisphere, equal area projections showing the basis of the SCI method. (a) Paleomagnetic dataset showing the paleomagnetic directions (before bedding correction, BBC) and their respective SCs. (b) The parameter  $A/n$  is the sum of all  $\alpha_i$  normalized by the number of sites and can be calculated for the directions susceptible to be the remagnetization direction. (c)  $A/n$  contour plot. The remagnetization direction corresponds with the minimum value of  $A/n$  (SCI solution). The ratio  $mr/me$  between the real and the possible number of intersection is also indicated. Paleomagnetic data come from remagnetized limestones (see [supplementary data](#)).

### Increasing the concentricity of the SCs

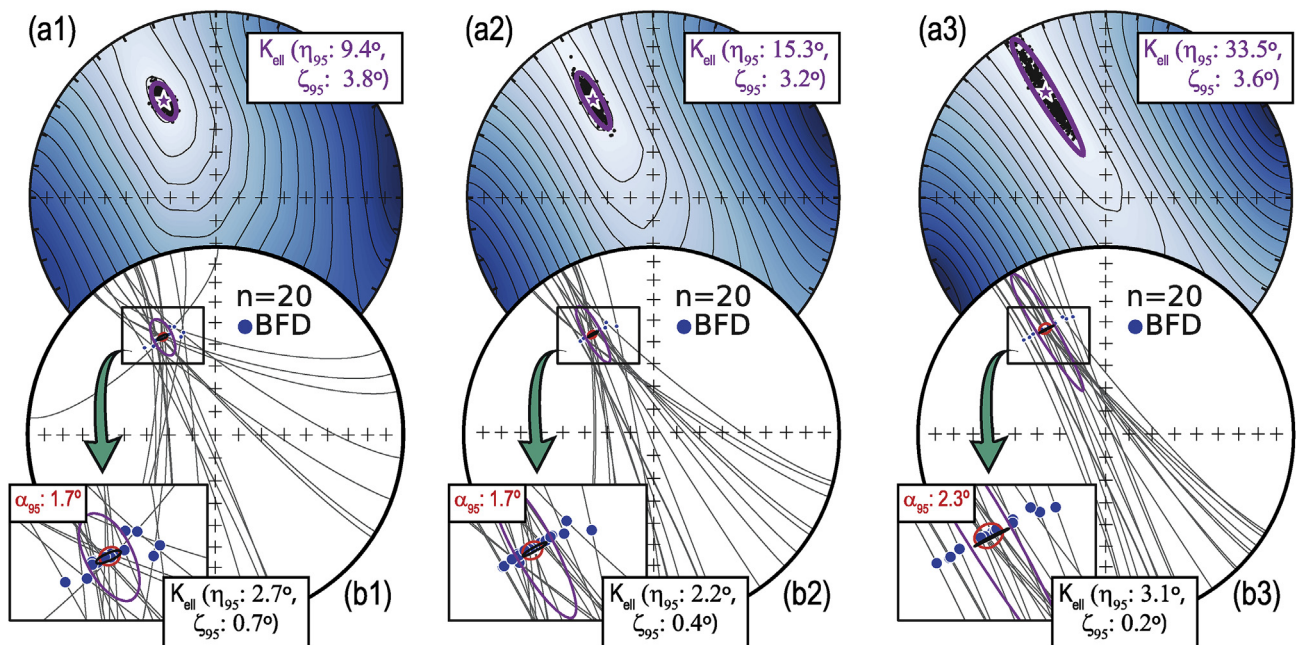


**Fig. 3.** (a)  $A/n$  contour plots obtained from three examples of SCI solution (star) from three different distributions of 20 SCs with different degree of concentricity. The calculated SCI solutions (small black points; i.e. different solutions considering the uncertainty coming from bedding and paleomagnetic data) and their 95% confidence ellipses and statistical parameters (Kent, 1982). (b) Equal area projections showing the three corresponding SC distributions and the best fit directions (BFD). 95% confidence circle (Fisher, 1953) and 95% confidence ellipse (Kent, 1982) corresponding to the 20 BFDs are depicted for comparison. Statistical parameters  $\alpha_{95}$  and maximum and minimum semi-angles ( $\eta_{95}$  and  $\zeta_{95}$ ) are also indicated. The used paleomagnetic dataset can be found in the [supplementary material](#).

provided a useful discussion about the uncertainties in the calculation of the paleomagnetic direction (a weak point in paleomagnetism in general, and in the SCI method, in particular).

Finally, Waldhör (1999) and Waldhör and Appel (2006) substantially improved the SCI method as a tool to calculate remagnetization directions. They discussed widely the applicability of the SCI method, focusing their work in testing it under different conditions, such as the distribution of the strike of the beds and the corresponding dispersion pattern of the intersections. In addition, these authors introduced the statistic  $A$ , the sum of the minimum angle between any direction and each SC. The direction minimizing  $A$  is assumed to be the

remagnetization direction. Moreover, the distribution of  $A$  values (or  $A/n$ , normalizing the  $A$  value for the number of sites  $n$ ) for all directions can be used as an indicator of dispersion of the SC distribution, or at least as an indicator of the reliability of the remagnetization direction.

Following this line of logic, an important concept is the best fit direction (BFD) which is the vector located along each SC closest to the calculated remagnetization direction. The angle between the BFD and the paleomagnetic direction for each site before bedding correction (BBC) is the unfolding angle (Villalaín et al., 2003) and the angle between the BFD and the paleomagnetic direction after total bedding correction (ATBC) is the paleodip of the bed (i.e. the dip of the beds to the moment of the

acquisition of the remagnetization). This was the workflow followed by Villalaín et al. (2003) who introduced the term of ‘asymmetrical solution’, consisting of differential unfolding of each limb depending of the calculated paleodip. Hence, the reconstruction of the beds through this method offers a unique image of the geological structures at the moment of the remagnetization.

Since its introduction, several investigators have presented different applications of the SC methods. Meijers et al. (2011) use it as a conventional fold test. Others use SC analysis for reconstructing the paleo-geometry of sedimentary basins (Villalaín et al., 2003; Soto et al., 2008, 2011; Casas et al., 2009; Torres-López et al., 2016), for separating deformation generated under different tectonic phases (Smith et al., 2006) or for relative dating of geological structures (Calvín et al., 2017). An extended review of the restoration methodology by using the SC methods (focused in intraplate basins) can be found in Villalaín et al. (2016). Promising results show also the applicability of the SCI method in geological frameworks with regional vertical axis rotations (VARs) generated after the acquisition of the remagnetization (e.g. Waldhör et al., 2001; Antolín et al., 2012; Rouvier et al., 2012). These VARs are added to the tilting recorded by the beds. In this context, and starting from the knowledge of an external paleomagnetic reference direction, it is possible to calculate the amount of tilting and VAR recorded by the rocks; however, more knowledge about the behavior of the SCs methods under tectonic frames affected by VAR is necessary to avoid misleading interpretations. Finally, another use derived from the calculation of the paleomagnetic direction is the dating of the remagnetization by comparison with the Apparent Polar Wander Path (APWP) in local coordinates (e.g. Henry et al., 2001; Gong et al., 2009; Torres-López et al., 2014). Needless to say that the presence of younger regional tilting or VARs will complicate this task (e.g. Jordanova et al., 2001).

In summary, the inherent uncertainty of the tectonic correction in synfolding remagnetizations makes analysis using the SC methods useful for inferring paleomagnetic directions. One of the main advantages of the SC methods for structural reconstructions based on synfolding remagnetizations lies in the fact that it does not assume proportional unfolding in each limb. Moreover, the SC offers the possibility of a graphical output allowing us to explore complex situations while minimizing possible “black-box” effects. These are two key points, while the classical and progressive fold-test can be used to check the primary or secondary origin of the magnetization, the SC methods have the potential for additional information. If the required external conditions for applying the methods are fulfilled (actually, or as a working hypothesis), they allow the calculation of the direction of a remagnetization, and of restoring each site separately to the moment of its acquisition.

The main problem for the application of the SC methods was the absence of software to do the necessary calculations in an straightforward way. Only two unpublished software packages, one of them written by B. Henry (IPGP, Paris) and another by M. Waldhör (UT, Tübingen) as an excel spreadsheet, have allowed application of the SCI method to paleomagnetic datasets, although they do not provide restoration utilities. Recently, the new version of VPD software (Ramón et al., 2017) also allows application of the SCI method. Therefore, although it is certain that many researchers are grateful for these programs, the absence of user-friendly, open source software has precluded widespread application of the SC methods and its regular use has been restricted to a few research groups (IPGP of Paris–France-, Tübingen University–Germany-, Burgos and Zaragoza Universities–Spain-).

In this paper, we present pySCu as the new Python-based software package which allows easy calculation of the remagnetization direction (SCI solution) for a dataset and provides the paleo-dip of each site (for bedding restoration) among other parameters. In this way, we propose (and we consider it necessary) the routine use of this method in magnetotectonic investigations in the same way that the classical fold test has been used traditionally. The software is based on the iterative method for calculating the remagnetization direction used in the previous software, especially Waldhör’s spreadsheet. In addition, pySCu provide an

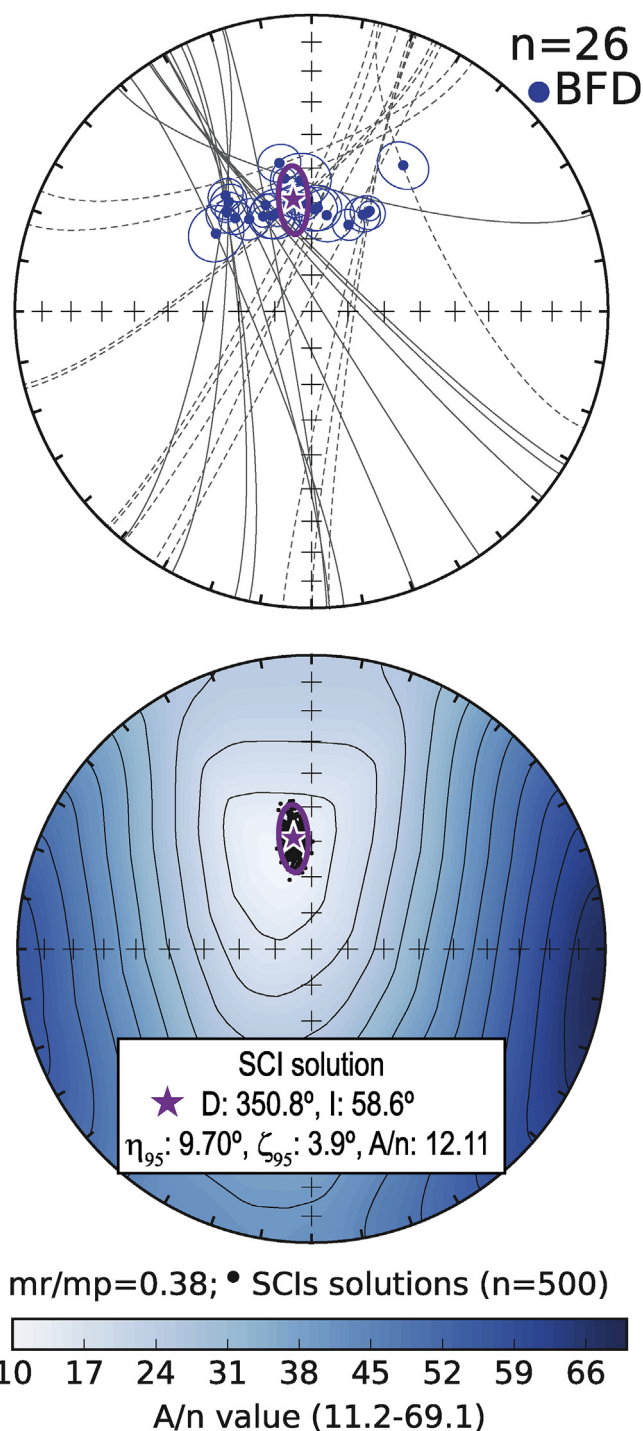
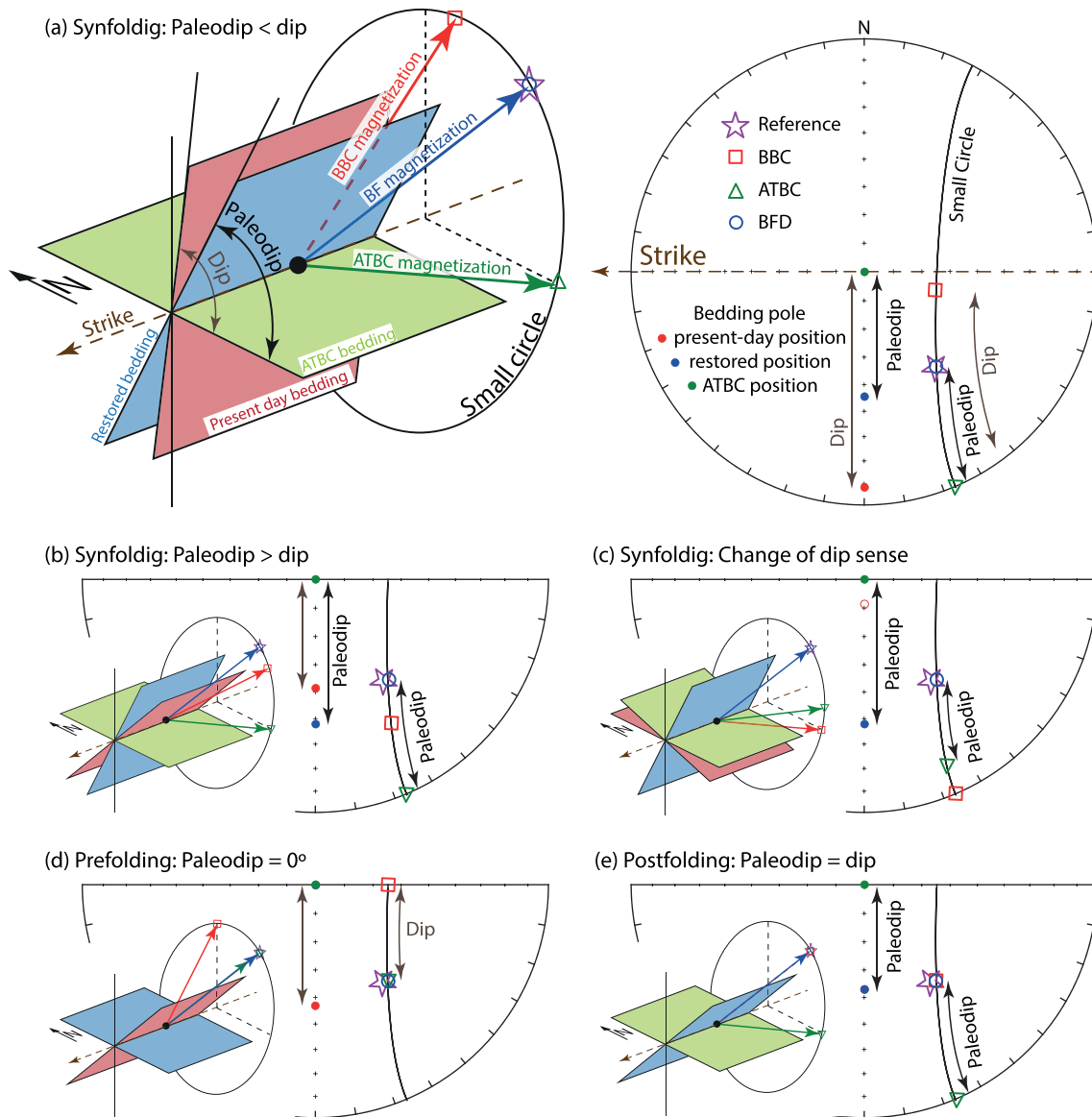


Fig. 4. Equal area projection showing the SCs and the best fit directions (BFD) of the same dataset shown in Fig. 2, in which some data (dashed SC) have been artificially rotated 50° according to a clockwise vertical axis rotation. Note that there are two concentrations of intersections corresponding with both populations easily identifiable by visual inspection. However, the contour plot of A/n shows a unique relatively well defined SCI solution. This is not correct because it is calculated from two datasets with different intersections as can be recognized in the SC distribution. In any case, by way of example of how to show the calculated SCI solution, it is shown together with the statistical parameters ( $\eta_{95}$  and  $\zeta_{95}$  are the major and minor semi-angles according Kent -1982- and A/n is the parameter introduced by Waldhör and Appel -2004-). The used paleomagnetic dataset can be found in the supplementary material.

uncertainty ellipse for the SCI solution on the basis of parametric bootstrapping techniques. Besides, it follows the philosophy of the new PmagPy software package (Tauxe et al., 2016) with open source code



**Fig. 5.** Different examples of paleodip restorations depending of relationship of timing between tilting and acquisition of the remagnetization: (a), (b) and (c) show synfolding remagnetizations with different tilting histories, (d) and (e) show pre-folding and post-folding remagnetization respectively. Each situation illustrates the relationship between bedding and paleomagnetic direction with a 3D sketch and in equal area projection. Red, blue and green correspond respectively with BBC, BFD and ATBD paleomagnetic directions. In equal area projection, solid symbols are represented in the lower hemisphere and hollow symbols in the upper one; note that the reference direction has negative inclination. (For interpretation of the references to colour in this figure legend, the reader is referred to the web version of this article.)

which can be easily modifiable for specific cases or for future improvements of the method; in fact, the drawing module (`pySCu_draw.py`) uses code from `PmagPy` to avoid repeating this code with the same aim.

## 2. Theoretical background

### 2.1. Definition of parameters

Small circles (SCs) are the key of the SC methods. One SC corresponds to the path followed by the paleomagnetic direction with progressive rotation around an axis parallel to the bedding strike (Fig. 1a). For each site, the SC is defined by the bedding strike ( $t$ , according to the right hand rule -RHR-) and the in situ magnetization (i.e. the SC that contains the magnetization and whose axis is  $t$ ) (Fig. 1a). Therefore, each SC can be parametrized by  $t$  and its apical angle  $Ap$  (or by  $d$ , the cosine of  $Ap$ , since calculations are performed on a unit sphere).  $Ap$  is the angle between the vector magnetization and the strike.

The program works by minimizing angular distances. For this

purpose, it must calculate the minimum angular distance ( $\alpha$ ) between different directions (P, directions susceptible of being the remagnetization direction, see next subsection) and each SC (Fig. 1b). The minimum angular distance  $\alpha$  is measured over a great circle that contains P and whose strike is  $t$  (Fig. 1b).

Once the angular distances between P and each SC have been calculated, the coordinates of the closest point to P located along the SCs are calculated. This point (Q) corresponds to the intersection between the SC and the great circle that contains P (Fig. 1b).

### 2.2. The remagnetization direction (SCI method)

The SCI method is based on the following assumptions. (i) The analyzed sites were remagnetized contemporarily and therefore they acquired the same remagnetization direction. (ii) Assuming, that only tilting of the bedding strike is responsible for the dispersion of the paleomagnetic direction from their original direction, the remagnetization direction must be placed upon the SC that links the paleomagnetic

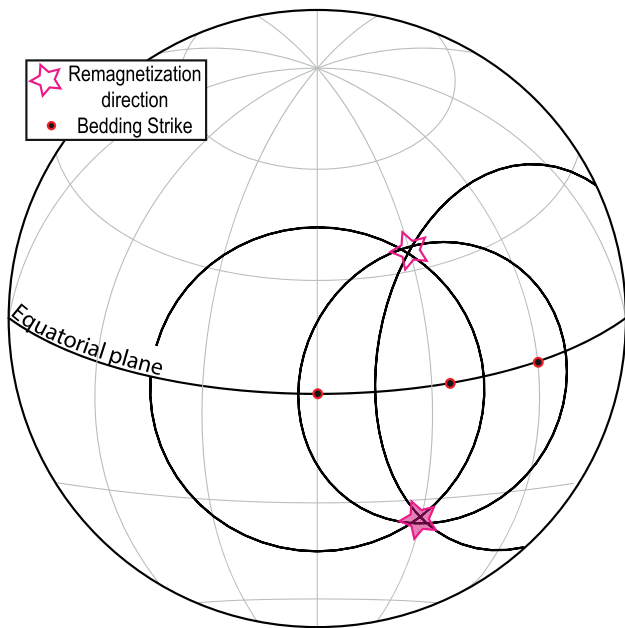


Fig. 6. Schmidt projection of a set of SCs showing the symmetry of the SCs between the upper and lower hemispheres and hence the two possible remagnetization direction having the same declination but opposite inclinations could be right.

Table 1

Example of input data file. Remember that this must be a comma separated text file. SITE: name of the site; rem D/rem I: in situ (BBC) declination and inclination of the remanence. alpha95 and kappa: semi-angle of the cone of confidence  $\alpha_{95}$  and k parameter (Fisher, 1953) associated to the paleomagnetic direction; Dipdir/Dip: Dip direction and dip of the bedding; k\_bed: k parameter (Fisher, 1953) associated to the bedding.

| SITE | rem D | rem I | alpha95 | kappa | Dipdir | Dip | k_bed |
|------|-------|-------|---------|-------|--------|-----|-------|
| St01 | 300.6 | 62.1  | 3.2     | 300.6 | 321    | 55  | 120   |
| St02 | 348   | 27    | 3.9     | 202.7 | 270    | 21  | 120   |
| St03 | 268   | 27    | 4.6     | 146.0 | 310    | 84  | 120   |

direction in BBC (before bedding correction) and ATBC (after total bedding correction) (Fig. 1a). If these two conditions are true, then it follows that all SCs should intersect in the remagnetization direction. For the method to work effectively, the beds must have different strikes because otherwise all SCs would be concentric with no intersection.

Because of the noise in data collection, intersections of SCs will be scattered, and the typical dataset (Fig. 2a) will show an area in which the intersections between the different SCs cluster. According to Waldh r and Appel (2006), one way to calculate the remagnetization direction is to try and find the direction that minimizes its angular distances to the set of SCs. For this, the minimum angle between any particular direction and the SCs ( $\alpha_j$ ) can be calculated (Fig. 1b); the value of  $A/n$ , which is the sum of all individual angles ( $\alpha_i$ ) normalized for the number of sites can be calculated ( $\frac{1}{n} \sum \alpha_j$ , Fig. 2b). The SCI solution will be the one with minimum  $A/n$  value (i.e. the closest direction to the set of SCs; Fig. 2c). Once the SCI solution is calculated this becomes in the reference and the final points Q converge to the best fit direction (BFD), the closest direction between each SC and the reference.

### 2.2.1. Uncertainty estimation

Estimating the uncertainty associated with the calculated remagnetization direction is a complex issue. The difficulty stems from several aspects, such as the homogeneity of the attitude of bedding (the greater the homogeneity the greater the uncertainty along the SCs), the relationship between the remagnetization direction and regional structural trend, the non-coaxial nature of the pre- and post-remagnetization deformation, and/or the quality of the bedding and paleomagnetic

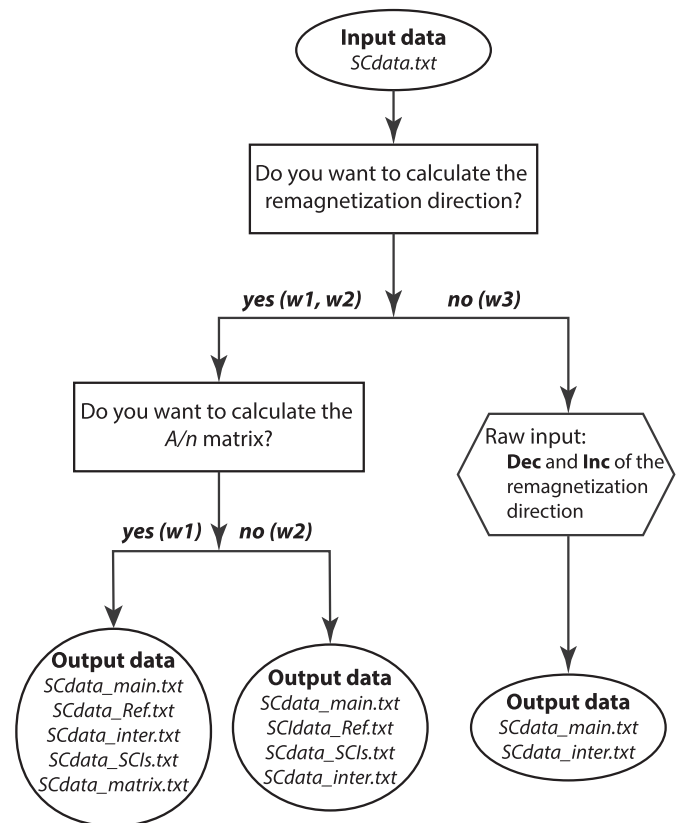


Fig. 7. Possible different workflows (w1, w2, and w3) within the pySCu\_calc.py module.

data. Given a SCI solution as in Fig. 2, the SC intersection pattern, as well as the  $A/n$  contour plot, gives a qualitative approximation of the uncertainty associated with the calculated direction; the uncertainty increases with the concentricity of the SCs and the eccentricity of  $A/n$  contours (Fig. 3a). However,  $A/n$  cannot be used as the regular confidence zones used in paleomagnetism with a quantitative statistical significance, precluding the use, for example, to compare with the apparent polar wander path for remagnetization dating. This issue has been traditionally assessed by means of Fisher (1953) statistics of the BFDs. This approach has two main flaws: (i) the BFDs do not usually follow a Fisherian distribution and (ii) these directions are artificially calculated (the BFD corresponds with the direction on each SC closest to the calculated direction which also invalidates non-Fisherian approach using the BFDs). As a consequence of this misuse, misleading confidence regions are obtained, and they tend to be elongated just in the direction perpendicular to the actual uncertainty (Fig. 3b); BFDs are forced in the uncertainty direction which is the same than the SC paths, and therefore they cannot show dispersion in this direction. Another consequence is that, whereas the real uncertainty of the solution increases with more concentric SC (magenta ellipse in Fig. 3), small variation can be observed between the confidence zones of the BFDs (red circle and black ellipse Fig. 3), indicating an absence of statistical significance of the latter.

Following an approach similar to Henry et al. (2004), the uncertainty of the SCI solution can be estimated by means of confidence areas with statistical significance if several solutions are calculated. This is possible if many pseudosamples of the input data (i.e. paleomagnetic directions and bedding) are generated through parametric bootstrap (Fisher et al., 1987; Watson and Enkin, 1993; Tauxe and Watson, 1994). Combining pairs of paleomagnetic directions and para-bedding, in each pseudosample, new bootstrapped-SCs can be defined and used to calculate new SCI solutions. If a large number of SCI solutions are calculated (e.g. more than 100), the confidence zone can be calculated. In agreement with the results obtained in the previous examples (Fig. 3), the

dispersion of the 500 SCI solutions follows an elliptical distribution; therefore, and following the work of Tauxe et al. (1991), Kent (1982) statistic is used to calculate the 95% confidence ellipse.

The pseudosamples generated by parametric bootstrap will follow the same Fisherian distribution than the input data (by design) and share Fisher (1953)  $k$  parameter. Therefore, since either the paleomagnetic direction and the bedding have an error defined by the Fisherian distribution with precision parameter  $k$  (for bedding a  $k$  of 120–150 can be realistic), the propagation of this error to the SCs can be introduced in the SCI solution in this way, which is exactly what this confidence region implies.

Even when used together with the confidence zone, the SCI solution can be unrealistic if some of the initial assumptions are not fulfilled. For example, if the SCI method is applied to a dataset affected by differential VAR, we will obtain wrong solutions even having reasonable  $A/n$  distributions and confidence zones (Fig. 4). For this, in our opinion, the best way to assess the uncertainty of the calculated remagnetization direction is through the confidence zone and the  $A/n$  value always accompanied with the SCs (or their intersections) and  $A/n$  values distribution (Fig. 4).

### 2.3. The paleodip calculations

The paleodip is the dip of the bedding plane at the moment of the acquisition of the remagnetization, obtained from simple calculations. (i) Once the reference is known, it is possible to calculate for each paleomagnetic site the direction within their corresponding SC closest to it, i.e. the BFD. (ii) The angle measured along the SC between the ATBC and the

BFD paleomagnetic directions corresponds with the paleodip (Fig. 5).

The frequently encountered situation working with synfolding remagnetizations is the one in which the paleodip shows an intermediate position between the BBC and ATBC attitudes (Fig. 5a), caused by a progressive tilting with the same sense along folding time (pre- and post-remagnetization tilting show the same dip direction). However, it is also possible to obtain opposite senses of tilting of the pre- and post-remagnetization stage, thus giving higher paleodips than present-day dips (Fig. 5b) or even changing the sense of dip of beds (Fig. 5c). In case of working with pre-folding remagnetizations, the paleodip will be 0° (Fig. 5d) and for post-folding remagnetizations the paleodip will coincide with the present-day dip (Fig. 5e). Real examples of these cases can be found in the literature (e.g. Smith et al., 2006; García-Lasanta et al., 2017; among others).

#### 2.3.1. The uncertainty in the paleodip

Uncertainty in the paleodip comes from the uncertainties in the bedding, in the paleomagnetic direction of each site and in the SCI solution. Bedding and paleomagnetic directions errors act at site-scale and the paleogeometry of the structures can be artificially modified. Therefore, the use of sites with high paleomagnetic direction uncertainties should be avoided, and just in case they can be used as a source of qualitative information. Besides, this uncertainty not only affects the magnitude of the  $\alpha_{95}$  of the paleomagnetic direction, but also the apical angle of the SC: for high apical angles (90° maximum), an  $\alpha_{95}$  of 5° will generate around 5° of paleodip uncertainty; however, for low apical angles (e.g. 20°), an  $\alpha_{95}$  of 5° will generate around 30° of paleodip

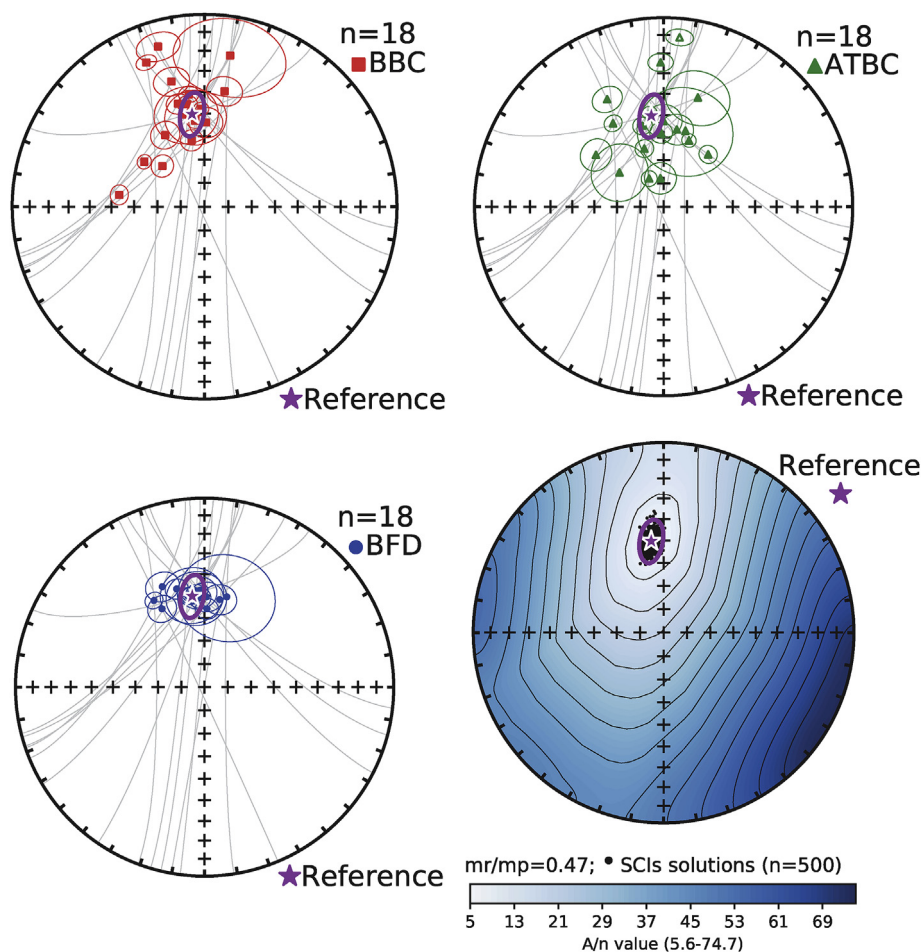


Fig. 8. Example of the output plots from pySCu\_draw.py. (a), (b), (c) show the SCs and BBC, BFD and ATBC paleomagnetic directions respectively. (d) Contour plot of  $A/n$ , the different calculated SCI solutions and their 95% confidence zone. Paleomagnetic data from Soto et al. (2011).

## Workflow of the iterative approach

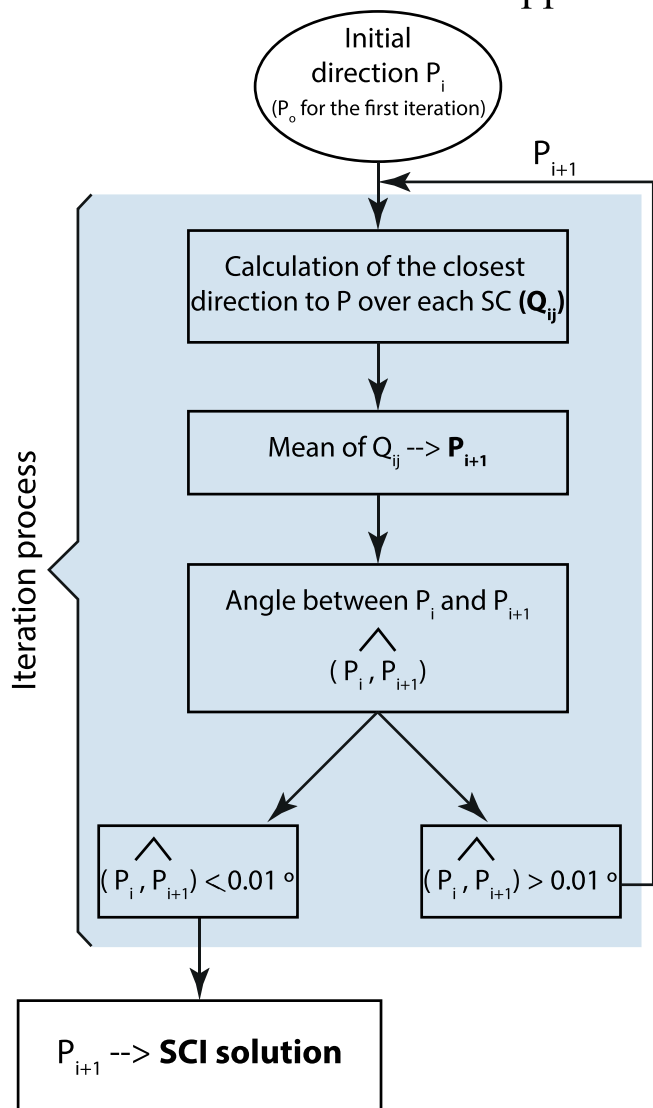


Fig. 9. Workflow followed by pySCu using the iterative approach. Given an initial direction  $P_0$ , the program starts the process with the calculation of all  $Q_{0j}$  points, and the mean of the calculated  $Q_{1j}$  directions (the  $Q_{1j}$  mean being transferred to the new point  $P_1$ ). In each iteration the angle between  $P_i$  and  $P_{i+1}$  is calculated. The iteration process goes on until the angle is lower than  $0.01^\circ$ . This process is repeated  $n$  times (500 by default) using a different *para*-dataset of SCs for calculating the different SCI solutions with which the 95% confidence zone is calculated.

uncertainty. Regarding uncertainties in bedding attitude, this is the same as for the dip and can be neglected for purposes of reconstruction of the structure.

Otherwise, the uncertainty in the SCI solution is common to all sites, and hence this will only affect the general attitude of the sites regarding an external reference, but will not affect the relative attitude between sites. In other words, the interlimb angle will be constrained, but the structures can be artificially tilted.

### 2.4. Considerations before using the SC methods

Some caveats must be taken into account when using the SC methods for calculating the reference direction and paleodips:

- There is an intrinsic ambiguity in the calculation of the reference direction (SCI solution), because it is always possible to calculate two remagnetization directions with the same declination and opposite

inclinations (Fig. 6). Other sources of information (e.g. paleomagnetic direction in horizontal sites) will be necessary to discriminate between both.

- For very similar strikes of bedding, the uncertainty in the calculated remagnetization direction will be high (Fig. 3b; e.g. Cairanne et al., 2002; Gong et al., 2009).
- Because the SCs methods works with remagnetization directions, we must be sure that we are working with a real remagnetization and not with an artifact, which can be generated by different processes. (i) Overlapping between two paleomagnetic components could be interpreted as a syn-folding remagnetization (Rodríguez-Pintó et al., 2013). (ii) Internal deformation of sedimentary beds can rotate a primary paleomagnetic components that shows the same behavior that a syn-folding remagnetization (e.g. Van der Pluijm, 1987; Stamatikos and Kodama, 1991). Anisotropy of the remanence measurements or sampling in different lithologies (e.g. limestones and marls) and therefore with different response to deformational mechanism can shed light to avoid these problems.
- The weight that each SC has in the SCI solution depends on the strike distribution (Waldhör and Appel, 2006). For example, in a case with several SCs defined by similar strikes and few SCs with axes at a high angle to the others, the remagnetization direction will be strongly conditioned by the latter.
- Generally, the SC methods are useful and reliable in contexts without complex tectonic histories (i.e. similar tilt axis during the pre- and post-remagnetization stages, Villalaín et al., 2016). Otherwise, in complex tectonic frames it can be necessary to restore the most recent deformation(s) before applying the SCs methods.
- In tectonic contexts with VAR postdating the remagnetization, the SCI method should be used with caution but it can still provide useful constraints (see Waldhör et al., 2001; Waldhör and Appel, 2006; Antolín et al., 2012; Rouvier et al., 2012). For example, it can be possible to assess the presence of differential VAR recorded by the different sites according to the SCs distribution, to calculate regional VAR if the paleomagnetic reference is known, etc.
- It is important to differentiate in these complex tectonic frames (last two points) between differential and regional VARs. The first will increase the noise in the calculated remagnetization direction and in the restoration. However, homogeneous VARs will preclude a right calculation of the remagnetization direction (and consequently its use for dating the remagnetization); structural relationship between sites will be accurate, but the general structures can be biased with respect to an external reference. In these complex tectonic frames external markers (e.g. geological markers) can help to avoid these effects. According to our experience, a large dataset can help minimizing the noise in the calculation of the remagnetization direction derived from anomalous strikes, uncontrolled sites with local VAR, etc.

The many caveats notwithstanding, it is worth noting that most of them are common to other paleomagnetic approaches applied to unravel the deformational history of the mountain belts, either working with primary or secondary remanences (e.g. Pueyo et al., 2016). Therefore the SC methods do not have more limitations than other techniques. In any case, it is a technique that works really well in simple tectonic frames, but also, combined with other methods, can help to understand complex deformational histories.

### 3. How to use pySCu

The pySCu program is written in Python 2.7 and consists of two different modules (each with their python file). pySCu\_calc.py is the main module which does the calculations and pySCu\_draw.py provides the graphical output for the program. This can be used either as a standalone software (downloading it from GitHub.com) or as a tool inside of the paleomagnetic set of tools PmagPy (Tauxe et al., 2016).

Following the first option (as an individual software), just search



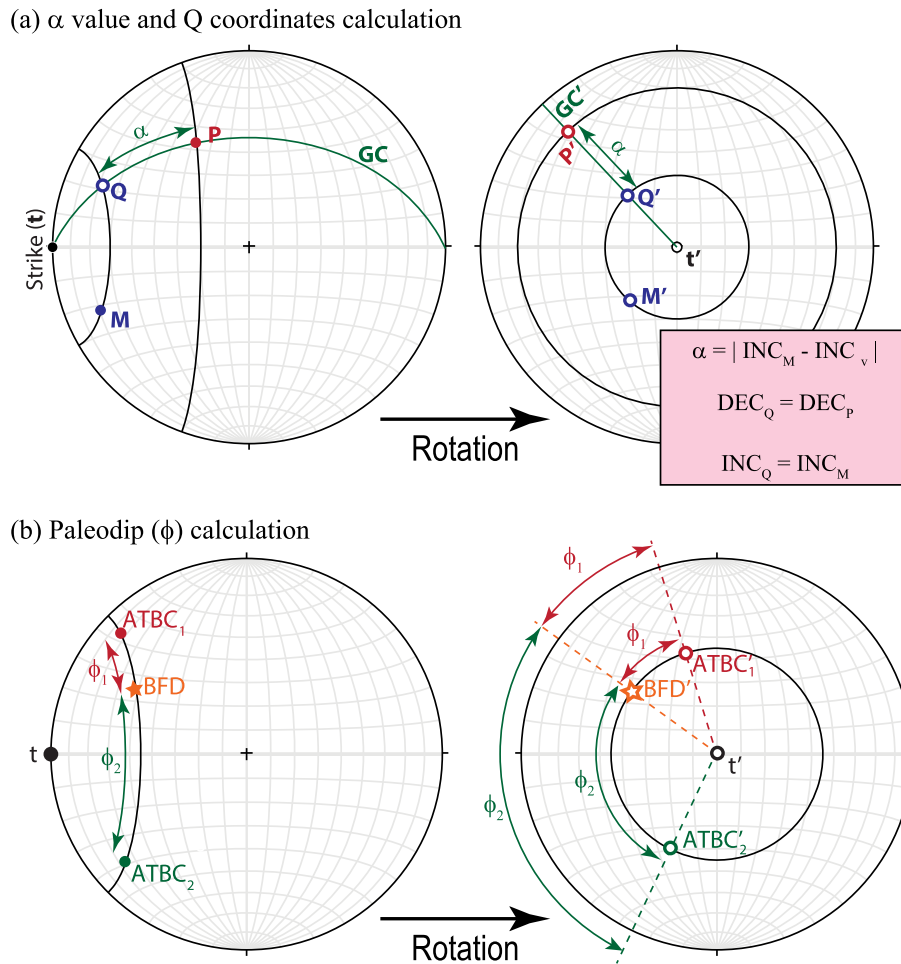


**Fig. 10.** (a) Equal area projection showing, as in Fig. 1, the relationship between P, M, Q and  $\alpha$  (abbreviations are the same than in previous figures and in the text). In the box, the calculations performed for calculating the  $\alpha$  value and the Q coordinates after the clockwise rotation of the elements looking to  $t + 90$ . (b) After the same clockwise rotation the paleodip ( $\phi$ ) can be calculated as a difference between declinations. Different possibilities exist depending on whether the sense of tilting between the pre- and post-remagnetization tilting is the same or opposite (elements 1 and 2 respectively).

pySCu in [www.GitHub.com](http://www.GitHub.com) webpage and download it (this also incorporates a 'readme' with the instructions). The program uses some basic Python libraries as Matplotlib-1.5.3 and Numpy-1.11.2 so it will not run on the standard Mac OS and Windows versions of python; we recommend either the Anaconda or Canopy installations. On the other hand, if you choose the PmagPy installation (which includes many other paleomagnetic tools), use pySCu as the other PmagPy's tools. The user is referred to the instructions for PmagPy and Anaconda or Canopy installations in the PmagPy cookbook at: <https://earthref.org/PmagPy/>.

### 3.1. pySCu\_calc.py

The input data file is a spaced delimited text file with header as shown in Table 1. All output data files (five as maximum) have this same format. Some communication with the program is necessary and it will be introduced through raw input.

The pySCu\_calc.py does different calculations: the parameters that define each SC, the possible intersections between each pair of SCs, the SCI solution and its confidence ellipse (through the calculation of 500 SCI solutions), the A/n matrix (a grid with the A/n values for all possible directions) and the paleodip for each site. These calculations can be performed following three different workflows (Fig. 7) depending on the user's requirements. (i) The basic step (w1, Fig. 7) is to do all calculations. (ii) Sometimes it can be interesting to quickly calculate remagnetization directions (w2, Fig. 7) using different datasets to assess the reliability of

some sites without calculating the A/n matrix (this takes some minutes). (iii) Finally, it is also possible to calculate the paleodips of the entire dataset using a remagnetization direction either calculated previously (SCI solution) or from other sources as the APWP (w3, Fig. 7a).

### 3.2. pySCu\_draw.py

The graphical output is mostly based on the PmagPy package (Tauxe et al., 2016). After running the program, it asks about the *\*main.txt* output file generated with pySCu\_calc.py. Then, a set of four equal area plots is generated (Fig. 8) representing the SCs, the BBC, BFD and ATBC paleomagnetic directions, the contour plot of the A/n, the 500 SCI solutions and the intersections of the SCs (the last three are optional). Besides, a modified version of this module is available (pySCu\_draw\_labels.py); this module draws only one equal area plot with the SCs, the reference direction, the BBC, BFD and ATBC paleomagnetic directions and the labels of the different sites. This is meant to use with few sites, for example for showing the results coming from a single fold.

Output plots from these modules are drawn with the matplotlib library and therefore they follow the design of this library. One important question is that this library allows saving the plots in different formats. The code of pySCu\_draw.py is easily modifiable to change the color, the size or the shape of the different elements as well as the configuration of the contour plot (just open it with a code editor).

## 4. How does pySCu work?

### 4.1. The iterative approach

The main workflow proceeds through an iterative approach (Fig. 9) in order to find the direction closest to the set of SCs, i.e. the SCI solution (Fig. 2). Given a starting point ( $P_0$ ), the program calculates, for each site, the closest direction ( $Q_{0j}$ ) over the  $SC_{0j}$  to the point  $P_0$ . When all  $Q_{0j}$  are known, their mean is calculated, defining the new reference point  $P_{i+1}$ . If the angular distance between  $P_i$  and  $P_{i+1}$  is higher than  $0.01^\circ$ , it is far from the solution and the process starts again using as a reference the new point  $P_{i+1}$ . Otherwise, if  $P_i$  and  $P_{i+1}$  are similar (angular distance between them smaller than  $0.01^\circ$ ), this means that  $P_i$  is the closest direction to all SCs (Fig. 8) and it becomes the SCI solution.

In practice, the program repeats this entire process 500 times, using each time a different pseudo-sample generated by parametric bootstrapping. For this, 30 new para-elements of bedding and BBC magnetization are generated at each site; the new families of para-elements have the same Fisherian distribution (same  $k$ ) than the input data. For each of the 500 repetitions of the iterative method, a pair of para-elements (bedding and BBC magnetization) is randomly chosen at each site to generate one different SC each time (see section 2.2.1). Once the program has calculated 500 SCI solutions, Kent (1982) statistic are apply to found the final SCI solution and the 95% confidence ellipse.

### 4.2. The $A/n$ matrix approach

The program calculates the remagnetization direction using the iterative approach, but in addition, it calculates the value of  $A/n$  for all possible directions (one-degree grid spacing). The end result is a contour plot of  $A/n$  which allows graphical analysis of the results. Both approaches must be convergent because they are based upon the same assumptions and same input data. However, there are some differences between them that explain why both are used in this program. The iterative approach is fast and allows calculating several SCI solutions for calculating the confidence ellipse. Conversely, the  $A/n$  approach takes a few minutes for calculating the  $A/n$  value for all directions (32,400 in total) but it provides a contour map of  $A/n$  values which gives us information about the reliability of the calculated paleomagnetic direction.

### 4.3. Some calculations

Except for the calculation of the  $d$  value and the apical angle of the SCs, pySCu uses an angle conversion for the rest of the calculations. The different elements presented in previous sections can be calculated by regular spherical trigonometry but due to the different situations regarding possible relationships between elements we decided to do the calculations starting from a  $90^\circ$  rotation of the reference system and consequently of all elements (the strike of the bed  $-t$ , SC, paleomagnetic vectors, etc.) around an axis perpendicular to the trend and in a clockwise sense (looking to  $t + 90^\circ$ ). Then: (i) the strike  $t$  becomes the vertical axis, and (ii) all elements placed the same SC will have the same inclination. In this way, all calculations can be done by scalar subtractions of declinations or inclinations (Fig. 10).

#### 4.3.1. $\alpha$ value and $Q$ coordinates

As indicated in the previous sections,  $\alpha_j$  is the minimum angular distance between  $P$  and a particular  $SC_j$  and it is measured along a great circle (GC) having the same strike that the SC. After the above mentioned  $90^\circ$  rotation of the cone axis, the plane represented by this great circle becomes vertical with the same declination than  $P$  (Fig. 10a) and therefore the angle  $\alpha$  corresponds to the difference in inclination between  $P$  and  $M$  vectors (in absolute value).

$Q_j$  is defined as the intersection between the great circle that contains  $P$  and whose strike is  $t$ . Therefore, after the rotation, the inclination of  $Q_j$

and  $M_j$ , on one side, and the declination of  $P_j$  and  $M_j$ , on the other, will be the same (Fig. 10a).

#### 4.3.2. Paleodip calculation

The paleodip is the dip of the bed when the remagnetization occurred. When the remagnetization direction is finally calculated,  $P$  becomes the reference for this particular bed (the remagnetization direction) and  $Q_j$  becomes the BFD (best fit direction), the theoretical paleomagnetic direction of the site at the moment of the remagnetization.

Since the actual dip of the beds is the angular distance (measured on the SC) between the BBC and ATBC paleomagnetic directions, the paleodip ( $\phi$ ) is the angle between BFD and ATBC paleomagnetic direction (Fig. 10b). This angle can be calculated from the dihedron between the planes defined by 1) the horizontal vector corresponding to the strike of the bed and the BFD for each plane on one side, and by 2) the bedding strike and the ATBC vector on the other. After the  $90^\circ$  rotation of the reference system, this calculation is simpler because it equals the angular difference of the declinations between ATBC and BFD vectors.

Some considerations regarding the relationship between the declination of the BFD and ATBC directions must be taken into account. According to the strike of the bed of the example shown in Fig. 10b, point 1 (ATBC<sub>1</sub>) agrees with a bed whose paleodip is between the present day paleodip and the horizontal (i.e. the pre- and post-remagnetization tilts have the same sense, see section 2.2), whereas point 2 (ATBC<sub>2</sub>) illustrates a bed whose paleodip has the opposite sense than the actual dip. This is important because the paleostrike (according to the RHR, right hand rule) will be the same than the strike for ATBC<sub>1</sub> but for ATBC<sub>2</sub> it will be the strike plus  $180^\circ$ . The program considers these situations for restoring the bed in the proper way.

## 5. Conclusions

When dealing with synfolding remagnetizations, the SC methods have several applications, such as performing detailed reconstructions of the attitude of each bed at the time of the remagnetization, calculating the local direction of the remagnetization or evaluating the presence of vertical axis rotations. All in all, one of the most important applications of the SC methods is that they allow graphical analysis of paleomagnetic datasets, avoiding possible “black-box” effects.

Application of parametric bootstrap allows us to assess the propagation of the error coming from the bedding and the paleomagnetic data. Working in this way it is possible to calculate the remagnetization direction together with its confidence ellipse.

Here the pySCu software, written in Python 2.7, for direct application of different SC applications is presented. It shows the advantage of being user-friendly, fast and easy, allowing a broader use of the SCI method in the paleomagnetic community, specifically applied to magnetotectonic studies using synfolding remagnetizations.

## Acknowledgments

This study was financed by the research projects CGL2012-38481 and CGL2016-77560 of the MINECO (Spanish Ministry of Economy and Competitiveness) with also FEDER founding (European Union). PC acknowledges the MINECO for the F.P.I. research grant BES-2013-062988. LT acknowledges support from National Science Foundation grant # EAR 1345003. The authors sincerely thank the constructive comments and suggestions of the reviewers Bernard Henry and Emilio L. Pueyo, which have helped to improve the SC methods and constrain their application limits.

## Appendix A. Supplementary data

Supplementary data related to this article can be found at <http://dx.doi.org/10.1016/j.cageo.2017.07.002>.

## References

- Antolín, B., Schill, E., Grujic, D., Baule, S., Quidelleur, X., Appel, E., Waldhör, M., 2012. E–W extension and block rotation of the southeastern Tibet: unravelling late deformation stages in the eastern Himalayas (NW Bhutan) by means of pyrrhotite remanences. *J. Struct. Geol.* 42, 19–33. <http://dx.doi.org/10.1016/j.jsg.2012.07.003>.
- Bazhenov, M.L., Shipunov, S.V., 1991. Fold test in paleomagnetism: new approaches and reappraisal of data. *Earth Planet. Sci. Lett.* 104, 16–24. [http://dx.doi.org/10.1016/0012-821X\(91\)90233-8](http://dx.doi.org/10.1016/0012-821X(91)90233-8).
- Cairanne, G., Aubourg, C., Pozzi, J.P., 2002. Syn-folding remagnetization and the significance of the small circle test examples from the Vocontian trough (SE France). *Phys. Chem. Earth* 27, 1151–1159. [http://dx.doi.org/10.1016/S1474-7065\(02\)00106-7](http://dx.doi.org/10.1016/S1474-7065(02)00106-7).
- Calvín, P., Casas-Sainz, A.M., Villalain, J.J., Moussaid, B., 2017. Diachronous folding and cleavage in an intraplate setting (Central High Atlas, Morocco) determined through the study of remagnetizations. *J. Struct. Geol.* 97, 144–160. <http://dx.doi.org/10.1016/j.jsg.2017.02.009>.
- Casas, A.M., Villalain, J.J., Soto, R., Gil-Imaz, A., del Río, P., Fernández, G., 2009. Multidisciplinary approach to an extensional syncline model for the Mesozoic Cameros Basin (N Spain). *Tectonophysics* 470, 3–20. <http://dx.doi.org/10.1016/j.tecto.2008.04.020>.
- Delanay, S., Smith, B., Aubourg, C., 2002. Asymmetrical fold test in the case of overfolding: two examples from the Makran accretionary prism (Southern Iran). *Phys. Chem. Earth, Parts A/B/C* 27, 1195–1203. [http://dx.doi.org/10.1016/S1474-7065\(02\)00130-4](http://dx.doi.org/10.1016/S1474-7065(02)00130-4).
- Fisher, R.A., 1953. Dispersion on a sphere. *Proc. R. Soc. Lond.* 217A, 295–305.
- Fisher, N., Lewis, T., Embleton, B., 1987. *Statistical Analysis of Spherical Data*. Cambridge University Press, Cambridge. <http://dx.doi.org/10.1017/CBO9780511623059>.
- García-Lasanta, C., Casas-Sainz, A., Villalain, J.J., Oliva-Urcia, B., Mochales, T., Speranza, F., 2017. Remagnetizations used to unravel large-scale fold kinematics: a case study in the Cameros basin (N Spain). *Tectonics*. <http://dx.doi.org/10.1002/2016TC004459>.
- Gong, Z., van Hinsbergen, D.J.J., Dekkers, M.J., 2009. Diachronous pervasive remagnetization in northern Iberian basins during Cretaceous rotation and extension. *Earth Planet. Sci. Lett.* 284, 292–301. <http://dx.doi.org/10.1016/j.epsl.2009.04.039>.
- Graham, J.W., 1949. The stability and significance of magnetism in sedimentary rocks. *J. Geophys. Res.* 54, 131–167. <http://dx.doi.org/10.1029/JZ054i002p00131>.
- Henry, B., Rouvier, H., Le Goff, M., 2004. Using syntectonic remagnetizations for fold geometry and vertical axis rotation: the example of the Cévennes border (France). *Geophys. J. Int.* 157, 1061–1070. <http://dx.doi.org/10.1111/j.1365-246X.2004.02277.x>.
- Henry, B., Rouvier, H., le Goff, M., Leach, D., Macquar, J.-C., Thibieroz, J., Lewchuk, M.T., 2001. Palaeomagnetic dating of widespread remagnetization on the southeastern border of the French Massif central and implications for fluid flow and Mississippi Valley-type mineralization. *Geophys. J. Int.* 145, 368–380. <http://dx.doi.org/10.1046/j.0956-540x.2001.01382.x>.
- Jordanova, N., Henry, B., Jordanova, D., Ivanov, Z., Dimov, D., Bergerat, F., 2001. Palaeomagnetism in northwestern Bulgaria: geological implications of widespread remagnetization. *Tectonophysics* 343, 79–92. [http://dx.doi.org/10.1016/S0040-1951\(01\)00220-7](http://dx.doi.org/10.1016/S0040-1951(01)00220-7).
- Kent, J.T., 1982. The Fisher-Bingham distribution on the sphere. *J. R. Stat. Soc. Ser. B* 44, 71–80.
- McCabe, C., Elmore, R.D., 1989. The occurrence and origin of Late Paleozoic remagnetization in the sedimentary rocks of North America. *Rev. Geophys.* 27, 471. <http://dx.doi.org/10.1029/RG027i004p00471>.
- McClelland-Brown, E., 1983. Palaeomagnetic studies of fold development and propagation in the Pembrokeshire old red sandstone. *Tectonophysics* 98, 131–149. [http://dx.doi.org/10.1016/0040-1951\(83\)90214-7](http://dx.doi.org/10.1016/0040-1951(83)90214-7).
- McFadden, P.L., 1990. A new fold test for palaeomagnetic studies. *Geophys. J. Int.* 103, 163–169. <http://dx.doi.org/10.1111/j.1365-246X.1990.tb01761.x>.
- Meijers, M.J.M., van Hinsbergen, D.J.J., Dekkers, M.J., Altöner, D., Kaymakçö, N., Langereis, C.G., 2011. Pervasive Palaeogene remagnetization of the central Taurides fold-and-thrust belt (southern Turkey) and implications for rotations in the Isparta angle. *Geophys. J. Int.* 184, 1090–1112. <http://dx.doi.org/10.1111/j.1365-246X.2010.04919.x>.
- Pueyo, E.L.L., Sussman, A.J.J., Oliva-Urcia, B., Cifelli, F., 2016. Palaeomagnetism in fold and thrust belts: use with caution. *Geol. Soc. Lond. Spec. Publ.* 425, 259–276. <http://dx.doi.org/10.1144/SP425.14>.
- Ramón, M.J., Pueyo, E.L., Oliva-Urcia, B., Larrasoña, J.C., 2017. Virtual directions in Paleomagnetism: a global and rapid approach to evaluate the NRM components. *Front. Earth Sci.* 5, 1–14. <http://dx.doi.org/10.3389/feart.2017.00008>.
- Rodríguez-Pintó, A., Pueyo, E., Barnolas, A., Pocolí, A., Oliva-Urcia, B., Ramón, M.J., 2013. Overlapped paleomagnetic vectors and fold geometry: a case study in the Balzes anticline (Southern Pyrenees). *Phys. Earth Planet. In.* 215, 43–57. <http://dx.doi.org/10.1016/j.pepi.2012.10.005>.
- Rouvier, H., Henry, B., Le Goff, M., 2012. Mise en évidence par le paléomagnétisme de rotations regionales dans la virgation des Corbières (France). *Bull. Soc. Geol. Fr.* 183, 409–424.
- Shipunov, S.V., 1997. Synfolding magnetization: detection, testing and geological applications. *Geophys. J. Int.* 130, 405–410. <http://dx.doi.org/10.1111/j.1365-246X.1997.tb05656.x>.
- Smith, B., Derder, M.E.M., Henry, B., Bayou, B., Yelles, A.K., Djellit, H., Amenna, M., Garces, M., Beamud, E., Callot, J.P., Eschard, R., Chambers, A., Aifa, T., Ait Ouali, R., Gandriche, H., 2006. Relative importance of the Hercynian and post-Jurassic tectonic phases in the Saharan platform: a palaeomagnetic study of Jurassic sills in the Reggane Basin (Algeria). *Geophys. J. Int.* 167, 380–396. <http://dx.doi.org/10.1111/j.1365-246X.2006.03105.x>.
- Soto, R., Villalain, J.J., Casas-Sainz, A.M., 2008. Remagnetizations as a tool to analyze the tectonic history of inverted sedimentary basins: a case study from the Basque-Cantabrian basin (north Spain). *Tectonics* 27. <http://dx.doi.org/10.1029/2007TC002208> n/a-n/a.
- Soto, R., Casas-Sainz, A.M., Villalain, J.J., 2011. Widespread Cretaceous inversion event in northern Spain: evidence from subsurface and palaeomagnetic data. *J. Geol. Soc. Lond.* 168, 899–912. <http://dx.doi.org/10.1144/0016-76492010-072>.
- Stamatatos, J., Kodama, K.P., 1991. Flexural flow folding and the paleomagnetic fold test: an example of strain reorientation of remanence in the Mauch Chunk formation. *Tectonics* 10, 807–819. <http://dx.doi.org/10.1029/91TC00366>.
- Suppe, J., 1983. Geometry and kinematics of fault-bend folding. *Am. J. Sci.* 283, 684–721. <http://dx.doi.org/10.2475/ajs.283.7.684>.
- Surmont, J., Sandulescu, M., Bordea, S., 1990. Mise en évidence d'une réaimantation fini crétacée des séries mésozoïques de l'unité de Bihor (Monts Apuseni, Roumanie) et de sa rotation horaire ultérieure. *Comptes Rendus L Acad. Des. Sci. Paris* 310, 213–219.
- Tauxe, L., Kylstra, N., Constable, C., 1991. Bootstrap statistics for paleomagnetic data. *J. Geophys. Res.* 96, 723–740.
- Tauxe, L., Watson, G.S., 1994. The fold test: an eigen analysis approach. *Earth Planet. Sci. Lett.* 122, 331–341. [http://dx.doi.org/10.1016/0012-821X\(94\)90006-X](http://dx.doi.org/10.1016/0012-821X(94)90006-X).
- Tauxe, L., Shaar, R., Jonestrask, L., Swanson-Hysell, N.L., Minnett, R., Koppers, A.A.P., Constable, C.G., Jarboe, N., Gaastra, K., Fairchild, L., 2016. PmagPy: software package for paleomagnetic data analysis and a bridge to the Magnetism Information Consortium (MagIC) database. *Geochem. Geophys. Geosystems* 17, 2450–2463. <http://dx.doi.org/10.1002/2016GC006307>.
- Torres-López, S., Villalain, J.J., Casas, A.M., EL Ouardi, H., Moussaid, B., Ruiz-Martínez, V.C., 2014. Widespread cretaceous secondary magnetization in the High Atlas (Morocco). A common origin for the Cretaceous remagnetizations in the western Tethys? *J. Geol. Soc. Lond.* 171, 673–687. <http://dx.doi.org/10.1144/jgs2013-107>.
- Torres-López, S., Casas, A.M., Villalain, J.J., El Ouardi, H., Moussaid, B., 2016. Pre-Cenomanian vs. Cenozoic folding in the High Atlas revealed by palaeomagnetic data. *Terra Nova* 28, 110–119. <http://dx.doi.org/10.1111/ter.12197>.
- Van der Pluijm, B.A., 1987. Grain-scale deformation and the fold test - evaluation of syn-folding remagnetization. *Geophys. Res. Lett.* 14 (2), 155–157. <http://dx.doi.org/10.1029/GL014i002p00155>.
- Villalain, J.J., Osete, M.L., Vegas, R., García-Dueñas, V., 1992. Evidencia de una reaimantación terciaria en la Béticas Occidentales. Implicaciones Tectónicas. *Física la Tierra* 4, 165–184.
- Villalain, J., Fernández-González, G., Casas, A.M., Gil-Imaz, A., 2003. Evidence of a cretaceous remagnetization in the Cameros basin (North Spain): implications for basin geometry. *Tectonophysics* 377, 101–117. <http://dx.doi.org/10.1016/j.tecto.2003.08.024>.
- Villalain, J.J., Casas-Sainz, A.M., Soto, R., 2016. Reconstruction of inverted sedimentary basins from syn-tectonic remagnetizations. A methodological proposal. *Geol. Soc. Lond. Spec. Publ.* 425, 233–246. <http://dx.doi.org/10.1144/SP425.10>.
- Waldhör, M., 1999. *The Small-circle Reconstruction in Palaeomagnetism and its Application to Palaeomagnetic Data from the Pamirs*. Tübingen University.
- Waldhör, M., Appel, E., 2006. Intersections of remanence small circles: new tools to improve data processing and interpretation in palaeomagnetism. *Geophys. J. Int.* 166, 33–45. <http://dx.doi.org/10.1111/j.1365-246X.2006.02898.x>.
- Waldhör, M., Appel, E., Frisch, W., Patzelt, A., 2001. Palaeomagnetic investigation in the Pamirs and its tectonic implications. *J. Asian Earth Sci.* 19, 429–451. [http://dx.doi.org/10.1016/S1367-9120\(00\)00030-4](http://dx.doi.org/10.1016/S1367-9120(00)00030-4).
- Watson, G.S., Enkin, R.J., 1993. The fold test in paleomagnetism as a parameter estimation problem. *Geophys. Res. Lett.* 20, 2135–2137. <http://dx.doi.org/10.1029/93GL01901>.